

1 **A Survey of Topsoil Arsenic and Mercury Concentrations Across France**

2 **B.P. Marchant^{a*}, N.P.A. Saby^b and D. Arrouays^b**

3 a: British Geological Survey, Keyworth, Nottingham, NG12 5GG, UK

4 b: INRA, US1106 Unité Infosol, Orléans, France

5 *: author for correspondence, benmarch@bgs.ac.uk

6 **Abstract**

7 Even at low concentrations, the presence of arsenic and mercury in soils can lead to ecological and
8 health impacts. The recent European-wide LUCAS Topsoil Survey found that the arsenic
9 concentration of a large proportion of French soils exceeded a threshold which indicated that
10 further investigation was required. A much smaller proportion of soils exceeded the corresponding
11 threshold for mercury but the impacts of mining and industrial activities on mercury concentrations
12 are not well understood. We use samples from the French national soil monitoring network (RMQS:
13 Réseau de Mesures de la Qualité des Sols) to explore the variation of topsoil arsenic and mercury
14 concentrations across mainland France at a finer spatial resolution than was reported by LUCAS
15 Topsoil. We use geostatistical methods to map the expected concentrations of these elements in the
16 topsoil and the probabilities that the legislative thresholds are exceeded. We find that, with the
17 exception of some areas where the geogenic concentrations and soil adsorption capacities are very
18 low, arsenic concentrations are generally larger than the threshold which indicates that further
19 assessment of the area is required. The lower of two other guideline values indicating risks to
20 ecology or health is exceeded in fewer than 5% of RMQS samples. These exceedances occur in
21 localised hot-spots primarily associated with mining and mineralization. The probabilities of mercury
22 concentrations exceeding the further assessment threshold value are everywhere less than 0.01 and
23 none of the RMQS samples exceed either of the ecological and health risk thresholds. However,
24 there are some regions with elevated concentrations which can be related to volcanic material,
25 natural mineralizations and industrial contamination. These regions are more diffuse than the hot-
26 spots of arsenic reflecting the greater volatility of mercury and therefore the greater ease with
27 which it can be transported and redeposited. The maps provide a baseline against which future
28 phases of the RMQS can be compared and highlight regions where the threat of soil contamination
29 and its impacts should be more closely monitored.

30 **Keywords**

31 Arsenic, mercury, topsoil, geostatistics, geogenic, contamination.

32 **Introduction**

33 Arsenic and mercury are toxic elements that can have negative effects on both ecosystems and
34 human health. Their presence in soil can lead to the degradation of water quality, to negative
35 impacts on the environment and to human health impacts through the contamination of water and
36 food. In comparison to other trace metals and metalloids, arsenic and mercury are relatively mobile
37 in the environment. Arsenic is susceptible to leaching in soil and although its vertical movements are
38 rather slow it is known to lead to contamination of groundwater (Meharg and Rahman, 2003).

39 Mercury is subject to volatilization at ambient temperatures and is hence prone to atmospheric
40 transport and deposition. Both metal(loid)s can be redistributed by erosion and accumulated in the
41 food chain. In a recent study, Tóth et al. (2016) studied the distribution of what they referred to as
42 heavy metal(loid)s in agricultural soils of the European Union. They compared the concentrations of
43 these elements observed in the LUCAS Topsoil Survey (Tóth et al., 2013) to thresholds (Table 1)
44 suggested by the Ministry of Environment of Finland (2007). Tóth et al. (2016) found a small
45 proportion of samples exceeded the threshold for mercury which indicated that further assessment
46 was required (0.5 mg/kg), and attributed these values to past gold mining activities. In contrast, they
47 found that a large proportion of samples across Europe exceeded the corresponding threshold for
48 arsenic (5 mg/kg). They therefore urged more focussed studies of the sources and distribution of
49 topsoil arsenic particularly in Spain, Italy and France. The analyses of Tóth et al. (2016) primarily
50 reported the metal(loid) concentrations at the scale of the European Union (EU) NUTS2 regions
51 (Eurostat, 2015). These are considered to be the basic regions for the application of regional policies.

52 Riemann et al. (In Press) suggested that the findings of Tóth et al. (2016) were rather alarmist and
53 noted that many of the threshold exceedances were as the result of the natural background
54 variation of geochemicals rather than contamination. The results of the GEMAS survey (Geochemical
55 Mapping of agricultural soils; Reimann et al., 2014) indicated that the continental-scale distribution
56 of many trace elements including arsenic (Tarvainen et al., 2013) and mercury (Ottesen et al., 2013)
57 were clearly dominated by geology. The dominant feature in maps of both elements was the
58 southern boundary of the former glacial cover. Larger concentrations were evident in the area
59 including France to the south of this line. Riemann et al. (In Press) therefore questioned whether
60 thresholds derived for Finnish soils, where lower concentrations would be expected, were
61 appropriate for the whole of Europe. For example, the soil action level for arsenic in agricultural soil
62 in Belgium is 45 mg/kg and in Germany the value is 50 mg/kg in soils with temporarily reducing
63 conditions and 200 mg/kg otherwise (Tarvainen et al., 2013). Similarly, Ottesen et al. (2013) noted
64 that the mercury action levels for sensitive land use in various countries vary between 1 and 23
65 mg/kg.

66 In an inventory of trace element inputs to French agricultural soils, Belon et al. (2012) demonstrated
67 that arsenic inputs from agricultural activities were not negligible. The inputs of mercury from such
68 activities were much smaller but their distribution due to mining and industrial activities and
69 atmospheric transport and deposition required investigation. Therefore, The French Agency for
70 Energy and Sustainable Development (Ademe), requested an assessment of the distribution of these
71 elements in mainland France, using the soil sample archive established by the French national soil
72 monitoring network (RMQS; Réseau de Mesures de la Qualité des Sols; Figure 1).

73 Since the RMQS is based on a systematic rather than probabilistic design, the set of observations of
74 each property cannot be treated as an independent sample and it is not possible to apply classical or
75 design-based statistical methods when analysing the data (Brus and De Gruijter, 1997). Instead, we
76 use model-based methods, specifically geostatistics, to model the spatial correlation between
77 observations and to account for the systematic design. Standard geostatistical models (e.g. Webster
78 and Oliver, 2007) include various assumptions about the observed data such that it is realized from a
79 second order stationary multivariate Gaussian random function. In general, environmental
80 properties do not conform to these assumptions. For example, the expected values of many soil
81 trace elements are non-stationary – they vary according to the geological setting or the rate of

82 deposition of the elements. Also, they are prone to extreme values or hot-spots that are inconsistent
83 with the Gaussian assumption. Therefore, we employ the trans-Gaussian linear mixed model (Diggle
84 and Ribeiro, 2007) to relax these assumptions and to produce reliable predictions of the spatial
85 variation of the concentrations of arsenic and mercury, to quantify the uncertainty of these
86 predictions and to determine the probability that the concentrations at each unobserved location
87 exceed legislative thresholds.

88 The linear mixed model divides the variation of the property of interest into fixed and random
89 effects. The fixed effects consist of a linear model relating the property to environmental covariates.
90 Knowledge of the processes controlling the spatial variation of the property can be included in the
91 model by selecting appropriate covariates. For example, we expect that the variation of arsenic and
92 mercury concentrations in French soils are influenced by the geological setting, inputs from
93 anthropogenic activities such as agriculture, industry and mining and the transport and deposition of
94 these elements from these sources. Therefore, the covariates we include, namely a classification of
95 parent material, a classification of land use, the average annual precipitation and the average annual
96 potential evapotranspiration reflect these processes. Having estimated our model, we use statistical
97 diagnostics to confirm that these covariates were indeed appropriate and significantly improved the
98 fit of the model.

99 Our objective is to assess how the concentrations of each element vary according to both natural
100 factors and anthropogenic factors. In addition, we want to provide a baseline against which future
101 phases of the RMQS can be compared and highlight regions where the threat of soil contamination
102 should be more closely monitored.

103 **Statistical Theory**

104 Model-based geostatistics treats $\mathbf{z} = [z(x_1), z(x_2), \dots, z(x_n)]^T$, the set of observations of a spatial
105 variable made at locations x_i , as if it was realised from a random function $Z(x)$. For example, the \mathbf{z}
106 might be assumed to be realized from a linear mixed model *i.e.*:

$$107 \quad \mathbf{z} = \mathbf{M}\boldsymbol{\beta} + \mathbf{r}, \quad (1)$$

108

109 where the $\mathbf{M}\boldsymbol{\beta}$ are the fixed effects and the \mathbf{r} are the random or residual effects. Each column of the
110 $n \times p$ matrix \mathbf{M} contains the values of a covariate at each of the n locations and the $p \times 1$ vector $\boldsymbol{\beta}$
111 contains regression coefficients. Often, all of the elements of the first column of \mathbf{M} are set equal to 1
112 so that the fixed effects include a constant. If a categorical property which classifies each location
113 into one of c classes (e.g. parent material classes) is included in the fixed effects then $c - 1$ columns
114 are added to \mathbf{M} . Each of these columns is a binary variable indicating the presence or absence of a
115 particular class at each location. The presence or absence of the remaining class can be deduced
116 from the presence or absence of these $c - 1$ classes. A continuous variable such as average annual
117 precipitation can be included in a single column of \mathbf{M} . Thus, the fixed effects are a linear model of p
118 covariates. The use of a linear mixed model is equivalent to the method referred to as kriging with
119 external drift (e.g. Webster and Oliver, 2007).

120 The $n \times 1$ vector of random effects is realized from a multivariate Gaussian random function with
121 mean zero and $n \times n$ covariance matrix \mathbf{C} . The elements of \mathbf{C} are determined from an authorised

122 variogram or covariance function $C(h)$ (Webster and Oliver, 2007) which describes how the
 123 expected squared difference between a pair of observations varies according to h , the distance
 124 separating the locations at which the observations were made. We use the nested nugget and
 125 Matérn covariance function:

$$126 \quad C(h) = \begin{cases} c_0 + c_1 & \text{if } h = 0 \\ c_1 G(h) & \text{for } h > 0 \end{cases} \quad (2)$$

127 where:

$$128 \quad G(h) = \frac{1}{2^{\nu-1} \Gamma(\nu)} \left(\frac{2\sqrt{\nu}h}{a} \right)^{\nu} K_{\nu} \left(\frac{2\sqrt{\nu}h}{a} \right), \quad (3)$$

129 Γ is the Gamma function and K_{ν} is a modified Bessel function of the second kind of order ν . The
 130 random effects model parameters are c_0 the nugget, c_1 the partial sill, a the distance parameter and
 131 ν the smoothness parameter. The inclusion of the smoothness parameter ν means that the Matérn
 132 function is flexible in terms of how $G(h)$ tends towards 1 for small h and it generalises some other
 133 commonly used covariance functions such as the exponential or Gaussian (Marchant and Lark,
 134 2007).

135 Often, the assumption of Gaussian random effects is not consistent with observations of trace
 136 elements in soil because the data include extreme values which correspond to geogenic or
 137 anthropogenic hot-spots (e.g. Marchant et al., 2011a). Indeed, the RMQS observations of arsenic
 138 and mercury (Figure 2 and Table 2) were highly skewed. Such behaviour can be accommodated in
 139 the spatial model by applying a transformation to the observed data prior to estimating the linear
 140 mixed model. We apply the Box Cox transformation:

$$141 \quad z_i = \begin{cases} \ln(y_i) & \text{if } \lambda = 0, \\ \frac{y_i^{\lambda} - 1}{\lambda} & \text{otherwise,} \end{cases} \quad (4)$$

142 where $y_i = y(x_i)$ is the observed concentration of the contaminant at location x_i , z_i is the
 143 corresponding transformed value which is assumed to be realized from the linear mixed model and
 144 λ is a parameter which gives the transformation some flexibility to ensure that the transformed
 145 values are consistent with a Gaussian distribution. Diggle and Ribeiro (2007) refer to such a model of
 146 a transformed variable as a trans-Gaussian model.

147 Our spatial model has p fixed effects parameters, four covariance function parameters and the Box
 148 Cox transformation parameter. Likelihood methods (Lark et al., 2006) can be used to fit all of these
 149 parameters to the observed data. A likelihood function quantifies the probability that the observed
 150 data would have been realized from a particular model with a specified set of parameters. The
 151 maximum likelihood estimator uses a numerical optimization procedure to find the set of parameter
 152 values that lead to the largest value of the likelihood.

153 The likelihood function can also be used to compare the suitability of different models. For example,
 154 we might wish to determine whether the inclusion of an additional covariate in the fixed effects
 155 leads to a worthwhile improvement in the fit of the model. The maximised likelihood from the
 156 extended model will be at least as large as the maximised likelihood from the original model. The
 157 Akaike Information Criterion (AIC; Akaike, 1973):

$$158 \quad AIC = 2k - 2L,$$

159 weighs the quality of fit or maximised log-likelihood L against the complexity or number of
160 parameters in the model k . The model with the smallest AIC is assumed to be the best compromise
161 between quality of fit and model complexity.

162 For a linear mixed model, there is known to be a small bias in the maximum likelihood estimate of
163 covariance parameters because the fixed effects parameters are treated as known rather than
164 uncertain values. Patterson and Thompson (1971) minimized this bias by using a residual maximum
165 likelihood (REML) estimator. The residual likelihood is not suitable for calculating the AIC.

166 Once the parameters have been estimated, the spatial model can be used to predict the expectation
167 \hat{Z}_t and variance \tilde{Z}_t of the random function $Z(x_t)$ at any target location x_t where the fixed effect
168 covariate information is available using the Best Linear Unbiased Predictor (BLUP). In the
169 geostatistics literature the BLUP is often referred to as the kriging predictor (Webster and Oliver,
170 2007). The spatial model can be validated by omitting a set of observations from the data set and
171 then using the remaining observations to predict the mean and variance of the random function at
172 the locations of the omitted observations. Then diagnostics such as the standardised squared
173 prediction error (SSPE):

$$174 \quad \theta_t = \frac{\{z_t - \hat{Z}_t\}^2}{\tilde{Z}_t}, \quad (5)$$

175

176 can then be calculated at each omitted site. If the prediction errors are Gaussian then the θ will be
177 realised from a standardised chi-squared distribution which has a mean of 1 and a median of 0.455
178 (Lark et al., 2006).

179 The Box Cox transformation must be inverted to determine the corresponding properties of the
180 random function of the observed concentration, $Y(x_t)$. If the inverse of Eqn. (4) is applied to a set of
181 predicted values of the expectation of $Z(x_t)$ then the median of $Y(x_t)$ results. The median of $Y(x_t)$
182 is not equal to the mean because the distribution of the random function is not symmetric. The
183 predicted mean of $Y(x_t)$ can be approximated by using the predicted mean and variance of $Z(x_t)$
184 to simulate a large number, e.g. 1000, realisations of $z(x_t)$. Then the inverse transformation is
185 applied to each simulated value to yield a simulated sample of $Y(x_t)$ and the mean of the random
186 function at this site can be predicted from the mean of this sample. The probability that $Y(x_t)$
187 exceeds a specified threshold at the target location can be approximated by the proportion of the
188 1000 back transformed simulated values which are larger than these threshold.

189 Further details regarding the estimation of and prediction from trans-Gaussian models are given by
190 Diggle and Ribeiro (2007). These authors also provide R software to implement these methodologies
191 (Ribeiro and Diggle, 2001).

192 **Methods**

193 *The French National Soil Monitoring Network (RMQS)*

194 The baseline survey of the RMQS (Arrouays et al., 2002) was completed in 2009. It consisted of
195 measurements of 40 properties of soil samples collected from the 2 200 nodes of a 16-km square
196 grid which covered the 550 000 km² French metropolitan territory (Figure 1). When factors such as
197 urban areas, rivers or roads prevented sampling on a particular node, a nearby (within 1 km)
198 cultivated or undisturbed location was sampled instead. When no such location was available, the

199 node was omitted. Such omitted nodes are evident in Figure 1; particularly in urban areas where
200 there is little bare soil.

201 At each sampled node, 25 individual soil cores were extracted according to an unaligned sampling
202 design within an area of 20×20m. Each core consisted of soil from depths of 0-30 cm. These depths
203 correspond to the layer of soil which in France is affected by ploughing. The individual cores were
204 bulked to form a composite sample of around 7 kg. Approximately 0.4 kg of each sample was used to
205 determine the 40 soil properties included in the initial protocol of the survey. The remainder of each
206 sample was stored in a purpose-built archive facility at the INRA research station in Orléans, France.

207 *Measurement of arsenic and mercury concentrations*

208 The arsenic and mercury concentrations were measured for each sample where sufficient soil
209 remained. The samples were prepared according to ISO 11464 (ISO, 2006). Each sample was dried at
210 a temperature not exceeding 40°C, and a homogenized portion was then crushed in a 2mm sieve. A
211 portion of this prepared soil sample was milled using a planetary ball mill machine. The subsample
212 was then sieved to 250 µm. Arsenic and Mercury were determined on this milled subsample.

213 Arsenic was determined after mineralization with a mixture of hydrofluoric acid and perchloric acid,
214 according to ISO 14869-1 (ISO, 2001). The mineralized solution was then analysed by mass
215 spectrometry coupled to argon induced plasma, using hydrogen/helium collision cell technology to
216 overcome interferences at mass 75. Dosages are performed on a Thermoscientific X series 2 ICPMS.

217 Mercury was analysed directly on the solid subsample, without preliminary mineralization, by a dry
218 combustion method under oxygen flow (AMA 254 Mercury Analyser). After the drying and
219 decomposition steps, the volatilized mercury was trapped and concentrated by a gold-based
220 amalgam. The latter was then briefly heated to a high temperature to release the mercury for
221 measurement by atomic absorption spectrometry. The test samples were between 20 and 200 mg
222 depending on the mercury content of milled soil subsample.

223 The quantification limits were 0.0025 mg/kg for mercury and 0.1 mg/kg for Arsenic. The INRA soil
224 analysis laboratory is accredited by COFRAC (the French accreditation committee) according to ISO
225 17025 (ISO, 2005).

226 *Statistical Analyses*

227 Trans-Gaussian linear mixed models were estimated for the spatial variation of arsenic and mercury
228 across mainland France. We hypothesised that the local geology, land use and the rate of deposition
229 were likely to be primary drivers of the variation in the concentrations of both elements. Therefore,
230 we considered including a parent material classification, a land use or land cover classification and
231 average annual precipitation as covariates in the fixed effects. Mean annual potential
232 evapotranspiration was also considered since mercury is known to be particularly sensitive to
233 volatilisation and strong evapotranspiration could reflect large mercury fluxes between the soil and
234 atmosphere. The parent material and land cover classifications were categorical variables with nine
235 and six classes respectively. Therefore, the inclusion of these covariates required a further 14
236 regression coefficients beyond the constant mean parameter which was also included. For each
237 element, we used the maximum likelihood estimator to calibrate the 16 linear mixed models
238 corresponding to the possible combinations of inclusion/exclusion of each of these four groups of

239 covariates. The AIC was used to select the most parsimonious model. The most appropriate model
240 for each element was then refitted using the REML estimator.

241 Leave-one-out cross-validation was performed for each fitted model and the resultant mean and
242 median SSPEs were compared to their theoretical values. The REML estimated models and the BLUP
243 were used to predict the concentrations of arsenic and mercury at each node of a 2-km square grid
244 which covered mainland French. The probability that the concentration of these elements exceeded
245 the thresholds proposed by the Ministry of Environment of Finland (2007) were also established. The
246 three classes of threshold for each element are shown in Table 1. The 'threshold value' indicates the
247 need for further assessment of the area. The 'guideline values' indicate concentrations which
248 present ecological or health risks. The higher guideline value applies at industrial and transport sites
249 whereas the lower guideline value applies elsewhere.

250 *Covariate Information*

251 The covariates considered for the fixed effects models are plotted in Figure 3 with a resolution of 1
252 km. The soil parent material information was extracted from the 1:1 000 000 scale soil database of
253 Europe (King et al., 1995). The classes in this database were merged into the nine classes shown in
254 Figure 3a. The land cover map was derived from the level three codes of the 2006 Corine land cover
255 map (European Environment Agency, 2010). These codes were amalgamated into six classes as
256 follows: 211-213 and 241-244 cropland; 231 grassland; 311-313 forest; 221-223 vineyard and
257 orchard; 111-142 urban and 321-523 other. These broader classes reflected the variation in the
258 natural content of geochemical trace elements (Atteia et al., 1994; Atteia et al., 1995; Baize, 1997;
259 Baize, 2007; Baize, 2009). The average annual precipitation was extracted from the WorldClim
260 dataset (<http://www.worldclim.org/>) and the average annual potential evapotranspiration was
261 extracted from the SAFRAN database (Quintana-Segui et al., 2008;
262 <http://www.cnrm.meteo.fr/spip.php?article424>).

263

264 **Results**

265 For arsenic, the best fitting model according to the AIC included parent material, land cover class,
266 mean annual precipitation and mean annual evapotranspiration in the fixed effects (Table 3). The
267 best fitting model for mercury included parent material, land cover class and mean annual
268 precipitation in the fixed effects (Table 4). The inclusion of the parent material, land cover and
269 precipitation covariates is consistent with our belief that there are both natural and anthropogenic
270 sources of these elements and that they are subject to transport and deposition. We expected that
271 the mean annual evapotranspiration was more like to be a driver of mercury variation than arsenic
272 variation since mercury is more sensitive to volatilisation. The exclusion of the evapotranspiration
273 term from the fixed effects of the mercury model possibly reflects that other confounding factors
274 are concealing the effect of mercury volatilisation.

275 For both elements, the mean standardised squared prediction errors upon cross-validation were
276 close to the theoretical value of 1.00. The median of the standardised squared prediction errors for
277 the best fitting arsenic model was 0.36 and the corresponding value for mercury was 0.31. These
278 values are reasonably close to the theoretical value of 0.45 and it appears that the models
279 adequately fit the data.

280 The variograms (Figure 4) for both elements have a substantial nugget component of around 50% of
281 the residual variance. The variograms differ in the effective range of spatial correlation. The effective
282 range is defined as the lag distance at which the spatially correlated component of the variogram is
283 equal to 95% of its sill variance. The arsenic variogram has an effective range of 238 km whereas the
284 mercury one has an effective range of 466 km. This leads to the map of estimated arsenic
285 concentrations having more localised hot-spots whereas regions of high mercury concentrations are
286 more diffuse (Figures 5 and 6). The probabilities of the concentrations exceeding the Ministry of
287 Environment of Finland thresholds are shown in Figure 7. In common with the results of the LUCAS
288 Topsoil Survey (Tóth, 2016), the concentrations of arsenic were considerably more likely to exceed
289 the threshold value than those of mercury. For much of France the probability of arsenic exceeding 5
290 mg/kg is greater than 0.9. The probability is slightly lower in the north of France and there are
291 regions in the south west and central France where the probability is close to zero. Generally, the
292 probability that the arsenic guideline values are exceeded (Figures 7c and 7d) are small except for
293 relatively isolated hot-spots. The probability of the mercury concentration exceeding its threshold
294 value is small across France only reaching 0.01 in hot-spots around Paris, along the border with Spain
295 and in the north east of the country. The probabilities of exceeding the mercury guideline values
296 (not shown) are negligible throughout France.

297 **Discussion**

298 The geographical regions and physical features of France referred to in this Discussion are shown in
299 Figure 8.

300 *Comparison with other surveys*

301 The RMQS, LUCAS Topsoil and GEMAS surveys differ in terms of their site sampling protocol and the
302 analytical methods used to determine arsenic and mercury concentrations. The LUCAS Topsoil
303 survey is restricted to agricultural soils and the GEMAS survey is restricted to agricultural and grazing
304 land (which are considered separately). The LUCAS Topsoil samples contain the top 20 cm of soil and
305 are extracted from five points on a 4m × 4m cross. The GEMAS samples are down to 20 cm for
306 agricultural land and 10 cm for grazing land and are the combination of five cores separated by
307 about 10 m. The LUCAS Topsoil survey has an average sampling density of 1 site/ 200 km², each land
308 use class in the GEMAS survey is sampled at a rate of 1 site/ 2500 km² whereas the 16 km grid of the
309 RMQS corresponds to a rate of approximately 1 site/250 km². The analytical methods for LUCAS
310 Topsoil and GEMAS were based on aqua regia extraction rather than the hydrofluoric acid extraction
311 used by RMQS. Aqua Regia is known not to extract the total amount of metalloids especially those
312 included in very resistant minerals. Therefore, we might have expected slightly higher
313 concentrations in the RMQS survey. However, the shallower sampling depth of the LUCAS Topsoil
314 and GEMAS surveys could be expected to lead to larger concentrations of mercury in regions where
315 it has been deposited in the soil surface. The larger spatial support of the RMQS samples might lead
316 to fewer extreme observations since very localised hot-spots will be more diluted.

317 The results of all three surveys indicate that for the majority of France there is a substantial
318 probability that the Ministry of Environment of Finland (2007) threshold value for arsenic is
319 exceeded. At the scale of the NUTS2 regions of the EU, between 30 and 90 % of the LUCAS Topsoil
320 samples from each region exceed this threshold. Our analyses (Figure 7a) indicate that for RMQS
321 samples the probabilities of exceedance are comparable and greater than 0.9 for a substantial

322 portion of the country. There are also clearly discernible areas in Figure 7a where the probability is
323 close to zero. These areas are not evident in the LUCAS Topsoil survey reporting at the NUTS2 scale.
324 The results of Tóth et al. (2016) indicate that the proportion of LUCAS topsoil samples exceeding
325 either the lower or upper guideline values for arsenic is less than 10 % in all of the NUTS2 regions.
326 The RMQS results (Figures 7c and 7d) are consistent with these findings although more localised
327 areas are evident where the probability of exceedance is up to 0.5.

328 The map of soil arsenic concentrations in Figure 6a is broadly similar to those derived by Tarvainen
329 et al. (2013). Tarvainen et al. (2013) list 53 arsenic anomalies across Europe, eight of which occur in
330 France. The French anomalies are primarily attributed to geology and mineralisation although
331 mining activities within the Massif Central and the use of pesticides to the south west of this region
332 are also cited. All of these anomalies are evident in Figure 6a apart from those associated with
333 pesticides which we discuss in the next section.

334 The mean and median observed concentrations of topsoil arsenic in France of approximately 12 and
335 18 mg/kg respectively (Table 2) are slightly smaller than the corresponding values of 15 and 20 and
336 mg/kg recorded in England and Wales (Rawlins et al., 2012) but larger than the median figure of 8
337 mg/kg reported by Reimann et al. (In Press) for the south of Europe. Although the results of our
338 analysis do indicate that, according to the Finnish threshold, further monitoring of topsoil arsenic
339 concentrations is required, it should be noted that that the largest RMQS measurements are
340 substantially less than those recorded at severely impacted sites such as former industrial areas in
341 the UK (Marchant et al. 2011b) and agricultural land neighboring industrial areas in China (Liao et al.,
342 2005) or in Bangladesh paddy soils where arsenic in groundwater used for irrigation contains large
343 amounts of arsenic (Meharg and Rahman, 2003).

344 The results of the LUCAS Topsoil and RMQS surveys agree that the probability that the soil mercury
345 concentration exceeds its threshold value is less than 0.1 across France. Tóth et al. (2016) do state
346 that “some soil samples with Hg above the higher guideline value (5 mg/kg) were still found on
347 agricultural land of France, Germany, Italy and Spain”. Such concentrations are substantially larger
348 than 1.37 mg/kg, the maximum value recorded in the RMQS. Such large values were not readily
349 apparent in the pictorial representations of the LUCAS Topsoil data in Tóth et al. (2016) where (in
350 agreement with Figure 6b) the mercury concentrations appear to be mostly in the range of 0.02-0.3
351 mg/kg. Therefore, these extreme values can be interpreted as localised outliers, perhaps caused by
352 localised soil contamination within the smaller spatial support of the LUCAS Topsoil samples.
353 Ottesen et al. (2013), reported that only 15 of the 4000 GEMAS samples returned mercury
354 concentrations greater than 1 mg/kg. They identified three mercury anomalies in France, namely
355 contamination from Paris, possible contamination from WW1 battlefields in Verdun and
356 mineralisation or contamination in the Vosges. The Paris and Vosges anomalies are evident in Figure
357 6b. The Verdun anomaly appears to be more localised although one elevated concentration in the
358 region is evident in Figure 1 (right). The RMQS median mercury concentration of 0.04 mg/kg is
359 similar to the corresponding GEMAS values for French agricultural and grassland displayed in Figure
360 4 of Ottesen et al. (2013). The Ottesen et al. (2013) maps of mercury concentrations across France
361 are broadly similar to Figure 6b although our results do appear to have a finer spatial resolution
362 reflecting the larger sampling density.

363 *The spatial variation of topsoil arsenic concentrations across France*

364 In Figures 5a and 6a we see that particularly small concentrations of topsoil arsenic are predicted in
365 sandy acidic soils such as in Landes, Sologne and North of the Vosges. These soils are developed on
366 deposits mainly composed of quartz, and the low concentrations result from very low geogenic
367 arsenic contents and very low adsorption capacities of the soils. There are also rather low
368 concentrations in the Paris Basin and more generally on the north-western part of France which is
369 characterized by the presence of quaternary eolian deposits (Arrouays et al., 2011). On a continental
370 scale, Tóth et al. (2016) found that areas of quaternary origin in the north of Europe have
371 substantially lower topsoil arsenic concentrations than most other regions. Moreover, most of these
372 soils developed on these deposits are luvisols characterized by a strong impoverishment of the
373 topsoil in clay and iron oxides. Shallow soils developed on chalk (Charentes, Champagne) also exhibit
374 rather low arsenic concentrations which might be attributable to the effects of high soil pH on
375 arsenic adsorption (Ghosh et al, 2006).

376 There are some localized arsenic hotspots (Vosges, Limousin, Cévennes, and borders of the Massif
377 Central). Previously, Bossya et al. (2012) commented on arsenic contamination within the Massif
378 Central. Some of these hotspots are correlated with well-known mining areas (e.g. the Limousin and
379 the Cévennes) and they are all places of intense geochemical mineralization. Since the majority of
380 the topsoil arsenic is contained in such hotspots there is a danger that the 16 km grid of the RMQS is
381 too coarse to fully capture the distribution of arsenic across France and some features might be
382 missed. For example, we observe quite large arsenic concentrations attributable to metallurgy and
383 coal mining in the north east (Lorraine) but we do not see the equivalent pattern in the north of
384 France, which has the same industrial history. Also, arsenic contamination might be expected in the
385 wine growing regions due to historic use of pesticides containing lead and arsenic. This pollution is
386 not evident in the predicted maps and might have been diluted by deep ploughing in the vineyards.

387 *The spatial variation of topsoil mercury concentrations*

388 There appear to be various natural and anthropogenic sources of mercury. The predicted maps
389 (Figures 5b and 6b) contain evidence of various geogenic effects linked to volcanic materials (centre
390 of the Massif Central) and some natural mineralizations in mountainous regions (Pyrénées, Jura,
391 Vosges, northern Alps and Massif Central). This effect may be amplified by the high levels of carbon
392 in these areas because mercury is strongly bound to organic matter (Ottesen et al., 2013; Wang et
393 al., 2015). Indeed, in Figure 9 we see that the lower bound on the mercury concentration within
394 RMQS samples does appear to increase with the concentration of soil organic carbon. These carbon
395 effects could also be leading to relatively high mercury concentrations in Brittany and Normandy for
396 instance.

397 There is a clear mercury contamination around Paris, that could be due to industrial smelting and
398 use of metals, waste burning, coal combustion for heating, and organic waste disposal on soil. One
399 hot spot in the north west of Paris almost exactly corresponds to the location of the biggest waste
400 water treatment plant in Europe and the second largest in the world. We might suspect that at this
401 site there has been a long history of organic waste spreading on the surrounding soils and that
402 historically the mercury contents in these wastes were not as well controlled as they are now
403 (Journal Officiel, 1980). There is also a smooth gradient of mercury towards the north and north-east
404 which is consistent with mercury transport by prevailing winds followed by re-deposition. This
405 transported mercury may directly come from historical industrial emissions or from volatilization

406 from soils surrounding old industries or having received contaminated urban sludge. Also, in the
407 extreme north of France, there is contamination that is attributable to the metallurgic industry.
408 Previous studies (e.g. Saby et al., 2011) have shown this region to be contaminated by cadmium,
409 lead and zinc and the residuals of coal burning. Finally, some hotspots of mercury in the Massif
410 Central region correspond to historical mining for gold.

411 **Conclusions**

412 National-scale soil monitoring networks are required to determine where soil functionality is
413 threatened and remediation or changes in land management practices might be required. It is not
414 always possible to anticipate the soil indicators that will be of interest to land managers and policy
415 makers. There are many threats to soil functionality such as erosion, decline in organic matter,
416 decline in biodiversity, contamination, sealing, landslides, salinization and compaction and the
417 priorities of stakeholders might change over time. Therefore, it is vital that soil samples are archived
418 so that different properties can be measured in the future. The RMQS archived a portion of soil from
419 each of the 2200 sites. This permitted us to measure the concentration of arsenic and mercury in
420 these samples, to determine the average concentrations of each element across France and to map
421 their spatial variation. Using linear mixed models and expert interpretation, we were able to identify
422 different origins of these metal(loid)s. Such relationships could not have been so easily discerned
423 had the modelling been restricted to a larger scale such as the EU NUTS2 regions. Arsenic came
424 principally from geogenic sources linked both to broad categories of soil parent material and to
425 more localized mineralization sources or mining activities. Mercury exhibited gradients linked to
426 human sources of diffuse contamination in addition to the effects of natural mineralization and
427 mining. Future phases of the RMQS will be compared to these baselines to determine whether and
428 where the concentrations of these toxic elements are increasing in French topsoils.

429 **Acknowledgements**

430 RMQS soil sampling and physico-chemical analyses were supported by a French Scientific Group of
431 Interest on soils: the "GIS Sol", involving the French Ministry for Ecology and Sustainable
432 Development (MEDD), the French Ministry of Agriculture (MAAP), the French Institute for
433 Environment, the Environment and Energy Management Agency (ADEME), the French Institute for
434 Research and Development (IRD), the National Geographic Institute (IGN) and the National Institute
435 for Agronomic Research (INRA). We thank all the soil surveyors and technical assistants involved in
436 sampling the sites. Soil analyses were performed by the central laboratory of INRA for soil (LAS, Inra
437 Arras, France). Ben Marchant's contribution was funded by the British Geological Survey (Natural
438 Environment Research Council) and published with the permission of the Executive Director of the
439 British Geological Survey (Natural Environment Research Council).

440 **References:**

441 Akaike, H., 1973. Information theory and an extension of the maximum likelihood principle. In:
442 Second International Symposium on Information Theory (eds B.N. Petrov and F. Csaki), pp 267-281,
443 Akadémiai Kiadó, Budapest.

444 Arrouays, D., Jolivet, C., Boulonne, L., Bodineau, G., Saby, N., Grolleau, E., 2002. A new initiative in
445 France: a multi-institutional soil quality monitoring network. *Comptes Rendus de l'Academie*
446 *d'Agriculture de France*, 88, 93–105.

447 Arrouays, D., Saby, N.P.A., Thioulouse, J., Jolivet, C., Boulonne, L., Ratié, C., 2011. Large trends in
448 French topsoil characteristics are revealed by spatially constrained multivariate analysis. *Geoderma*,
449 161, 107–114.

450 Atteia, O., Dubois, J., Webster, R., 1994. Geostatistical analysis of soil contamination in the Swiss
451 Jura. *Environ. Environmental Pollution*, 86, 315–327.

452 Atteia, O., Thelin, P., Pfeifer, H.R., Dubois, J.P., Hunziker, J.C., 1995. A search for the origin of
453 cadmium in the soil of the Swiss-Jura. *Geoderma*, 68, 149–172.

454 Baize, D., 1997. Teneurs totales en éléments traces métalliques dans les sols (France). Références et
455 stratégies d'interprétation. INRA Editions, Paris, 410 pp.

456 Baize, D., 2007. Teneurs en huit éléments en traces (Cd, Cr, Cu, Hg, Ni, Pb, Se, Zn) dans les sols
457 agricoles en France. Résultats d'une collecte de données à l'échelon national. Contrats n° 0375C0035
458 et 0575C0055, ADEME, Angers.

459 Baize, D., 2009. Cadmium in soils and cereal grains after sewage-sludge application on French soils. A
460 review. *Agronomy for Sustainable Development*, 29(1): 175–184.

461 Belon, E., Boisson, M., Deportes, I.Z., Eglin, T.K., Feix, I., Bispo, A.O., Galsomies, L., Leblond, S.,
462 Gueiller, C.R., 2012. An inventory of trace element inputs to French agricultural soils. *Science of the*
463 *Total Environment*, 439, 87–95.

464 Bossya, A., Grosbois, C., Hendershot, W., Beauchemin, S., Crouzete, C., Bril, H., 2012. Contributions
465 of natural arsenic sources to surface waters on a high grade arsenic-geochemical anomaly (French
466 Massif Central). *Science of the Total Environment*, 432, 257–268.

467 Brus, D.J., De Gruijter, J.J., 1997. Random sampling or geostatistical modelling? Choosing between
468 design-based and model-based sampling strategies for soil (with Discussion). *Geoderma*, 80, 1–44.

469 Diggle, P.J., Ribeiro, P.J., 2007. *Model-based Geostatistics*. Springer, New York.

470 European Environment Agency, 2010. Corine land cover 2006 raster data.
471 <http://www.eea.europa.eu/data-and-maps/data/corine-land-cover-2006-raster> (last accessed
472 November 2016).

473 Eurostat, 2015. NUTS – nomenclature of territorial units for statistics. Eurostat;
474 <http://epp.eurostat.ec.europa.eu/> (last accessed November 2016).

475 Ghosh, A., Sáez, A.E., Ela, W.P., 2006. Effect of pH, competitive anions and NOM on the leaching of
476 arsenic from solid residuals. *Science of the Total Environment*, 363, 46–59.

477 ISO, 2001. Reference ISO 14869-1: Soil quality - Dissolution for the determination of total element
478 content - Part 1: Dissolution with hydrofluoric and perchloric acids. International Organisation for
479 Standardization.

480 ISO, 2005. Reference ISO 17025:2005: General requirements for the competence of testing and
481 calibration laboratories. International Organisation for Standardization.

482 ISO, 2006. Reference ISO 11464:2006(E): Soil quality - Pretreatment of samples for physico-chemical
483 analysis. International Organisation for Standardization.

484 Journal Officiel, 1980. Décret n° 80-478 du 16 juin 1980 modifié portant application des articles
485 L.214-1 et L.214-2 du Code de la Consommation en ce qui concerne les matières fertilisantes et les
486 supports de culture (Journal officiel du 29 juin 1980; France), in French.

487 Lark, R.M., Cullis, B.R., Welham, S.J., 2006. On spatial prediction of soil properties in the presence of
488 a spatial trend: the empirical best linear unbiased predictor (E-BLUP) with REML. *European Journal*
489 *of Soil Science*, 57, 787–799.

490 Liao, X-Y., Chen, T-B, Xie, H., Liu, Y-R., 2005. Soil As contamination and its risk assessment in areas
491 near the industrial districts of Chenzhou City, Southern China. *Environment International*, 31, 791–
492 798.

493 Marchant, B.P., Lark, R.M., 2007. The Matérn variogram model: Implications for uncertainty
494 propagation and sampling in geostatistical surveys. *Geoderma*, 140, 337–345.

495 Marchant, B.P., Saby, N.P.A., Jolivet, C.C., Arrouays, D., Lark, R.M., 2011a. Spatial prediction of soil
496 properties with copulas. *Geoderma*, 162, 327–334.

497 Marchant, B.P., Tye, A.M., Rawlins, B.G., 2011b. The assessment of point-source and diffuse soil
498 metal pollution using robust geostatistical methods: A case study in Swansea (Wales, UK). *European*
499 *Journal of Soil Science*, 62, 346–358.

500 Meharg, A.A., Rahman Md.M., 2003. Arsenic Contamination of Bangladesh Paddy Field Soils:
501 Implications for Rice Contribution to Arsenic Consumption. *Environmental Science and Technology*,
502 37, 229–234.

503 Ministry of the Environment, Finland, 2007. Government decree on the assessment of soil
504 contamination and remediation needs (214/2007, March 1, 2007).

505 Ottesen, R.T., Birke, M., Finne, T.E., Gosar, M., Locutura, J., Reimann, C., Tarvainen, T., The GEMAS
506 Ptoject Team, 2013. Mercury in European agricultural and grazing land soils. *Applied Geochemistry*,
507 33, 1–12.

508 Patterson, H.D., Thompson, R., 1971. Recovery of inter-block information when block sizes are
509 unequal. *Biometrika*, 58, 545–554.

510 Quintana-Seguí, P., Le Moigne, P., Durand, Y., Martin, E., Habets, F., Baillon, M., Canellas, C.,
511 Franchisteguy, L., Morel, S., 2008. Analysis of Near-Surface Atmospheric Variables: Validation of the
512 SAFRAN Analysis over France. *Journal of Applied Meteorology and Climatology*, 47, 92–107.

513 Rawlins, B. G., McGrath, S. P., Scheib, A. J., Breward, N., Cave, M., Lister, T. R., Ingham, M., Gowing,
514 C., Carter, S., 2012. The Advanced Soil Geochemical Atlas of England and Wales. (Keyworth,

515 Nottingham: British Geological Survey.) <http://www.bgs.ac.uk/gbase/advSoilAtlasEW.html> (last
516 accessed December 2016).

517 Reimann, C., Négrel, P., Ladenberger, A., Birke, M., Filzmoser, P., O'Connor, P., Demetriades, A., In
518 Press. Comment on "Heavy metals in agricultural soil of the European Union with implications for
519 food safety" by Tóth, G., Hermann, T., Da Silva, M.R. and Montanarella, L. Environment International
520 <http://dx.doi.org/10.1016/j.envint.2016.07.019> (last accessed, December 2016).

521 Reimann, C., Birke, M., Demetriades, A., Filzmoser, P., O'Connor, P. (Eds.) 2014. Chemistry of
522 Europe's Agricultural Soils – Part A: Methodology and Interpretation of the GEMAS Data
523 SetGeologisches Jahrbuch (Reihe B 102). Schweizerbarth, Stuttgart 528 pp.

524 Ribeiro Jr, P.J. and Diggle, P.J., 2001. GeoR: A package for geostatistical analysis. R-News, vol. 1, No 2,
525 ISSN 1609-3631.

526 Saby, N.P.A., Marchant, B.P., Lark, R.M., Jolivet, C.C, Arrouays, D., 2011. Robust geostatistical
527 prediction of trace elements across France. Geoderma, 162, 303–311.

528 Tarvainen, T., Albanese, S., Birke, M., Poňavič, Reimann, C., The GEMAS Project Team, 2013. Arsenic
529 in agricultural and grazing land soils of Europe. Applied Geochemistry, 28, 2–10.

530 Tóth, G., Hermann, T., Da Silva, M.R., Montanarella, L., 2016. Heavy metals in agricultural soils of the
531 European Union with implications for food safety. Environment International, 88, 299–309.

532 Tóth, G., Jones, A., Montanarella, L., 2013. LUCAS Topsoil Survey – methodology, data and results.
533 EUR 26102 EN. Office for Official Publications of the European Communities, Luxembourg, p. 141.

534 Wang, X., Liu, X., Han, Z., Jian, Z., Xu, S., Zhang, Q., Haijie, C., Bo, W., Xia, X., 2015. Concentration and
535 distribution of mercury in drainage catchment sediment and alluvial soil of China. In: A.
536 Demetriades, M. Birke, S. Albanese, I. Schoeters, B. De Vivo (Guest Editors), Continental, Regional
537 and Local scale Geochemical Mapping. Special Issue, Journal of Geochemical Exploration, 154, 32–
538 48.

539 Webster, R. and Oliver, M.A., 2007. Geostatistics for Environmental Scientists, 2nd edition, John
540 Wiley & Sons, Chichester.

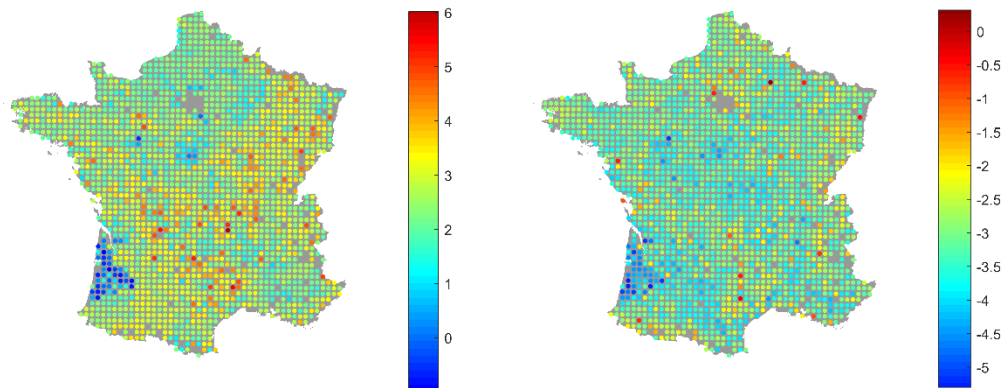
541

542

543

544

545 **Figures**

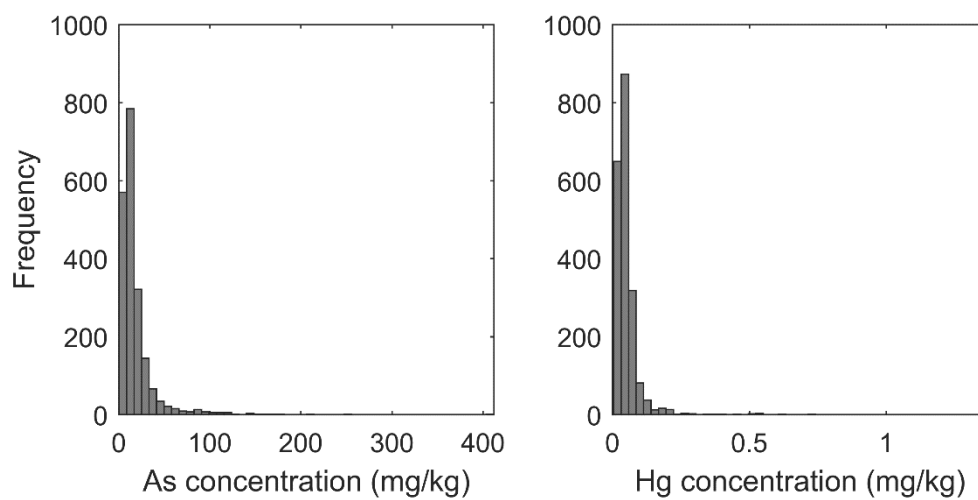


546

547 **Figure 1:** (Left) Observed values of the natural logarithm of the arsenic concentration (log mg/kg)
548 and (right) observed values of the natural logarithm of the mercury concentration (log mg/kg)
549 superimposed on the prediction grid with spacing 2 km (grey).

550

551

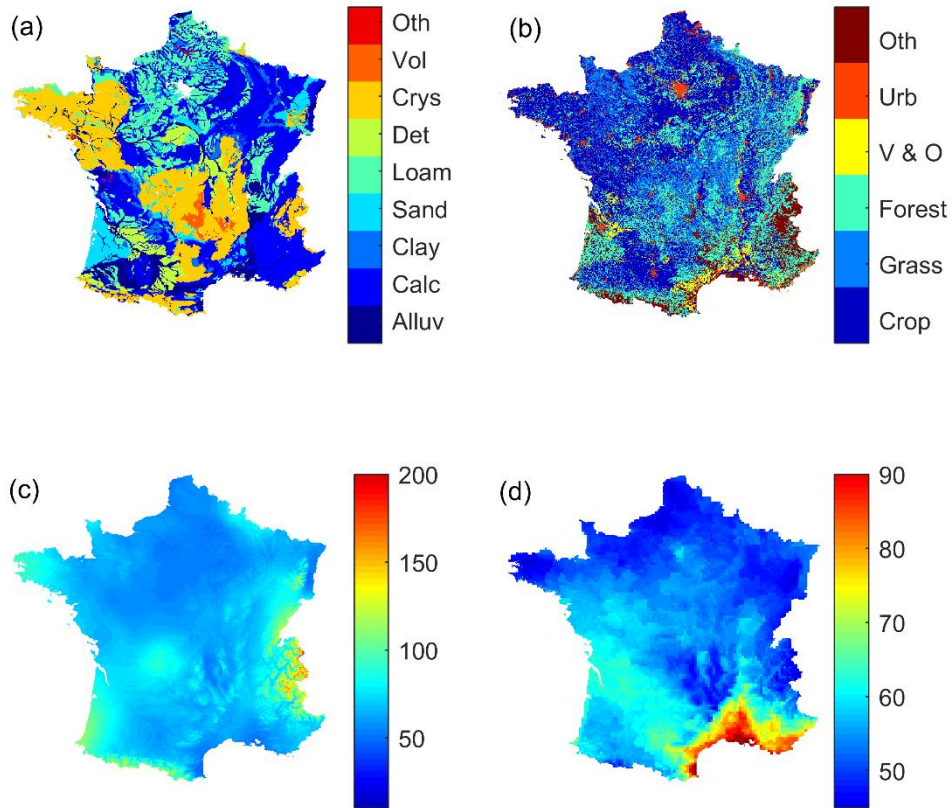


552

553

554 **Figure 2:** (left) Histogram of observed arsenic concentrations (mg/kg); (right) histogram of observed
555 mercury concentrations (mg/kg).

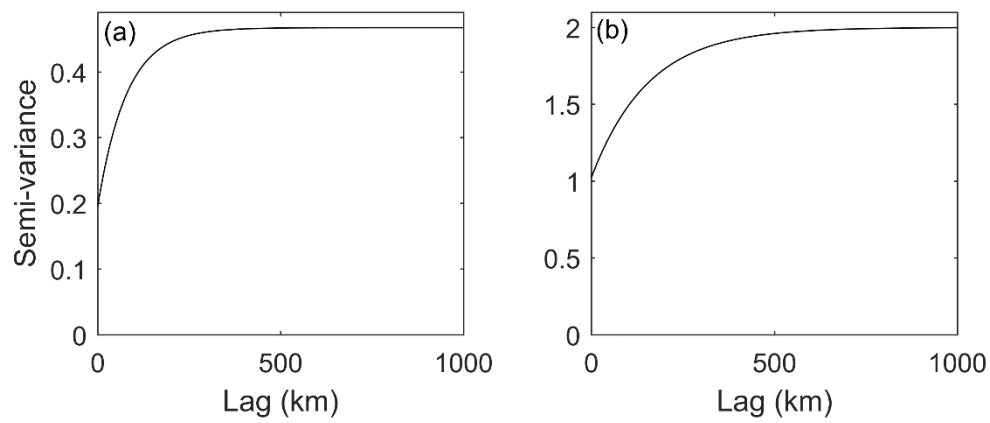
556



558

559 **Figure 3:** The spatial covariates included in the linear mixed model. (a) Parent material classes:
 560 “undifferentiated alluvial deposits or glacial deposits” (alluv); “calcareous rocks” (calc); “Clayey
 561 materials” (clay); “sandy materials” (sand); “loamy materials” (loam); “detrital formations” (det);
 562 “crystalline rocks and migmatites” (crys); “volcanic rocks” (vol) and “other rocks” (oth). (b) Land
 563 cover classes derived from the 2006 Corine land cover map: “cropland” (crop); “grassland” (grass);
 564 “forest” (forest); “vineyards and orchards” (V & O); “urban” (urb); “other” (oth). (c) Average annual
 565 precipitation (cm/year). (d) average annual potential evapotranspiration (cm/year).

566

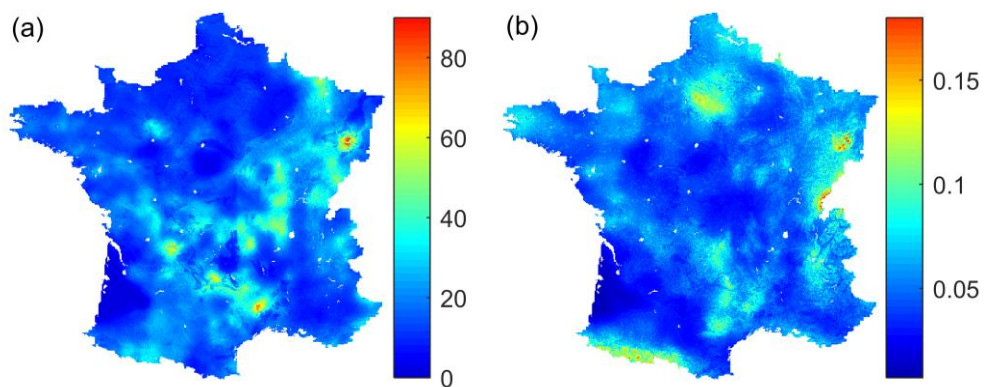


568

569 **Figure 4:** (a) estimated variogram of random effects from the linear mixed model of transformed
570 arsenic concentrations; (b) estimated variogram of random effects from the linear mixed model of
571 transformed mercury concentrations.

572

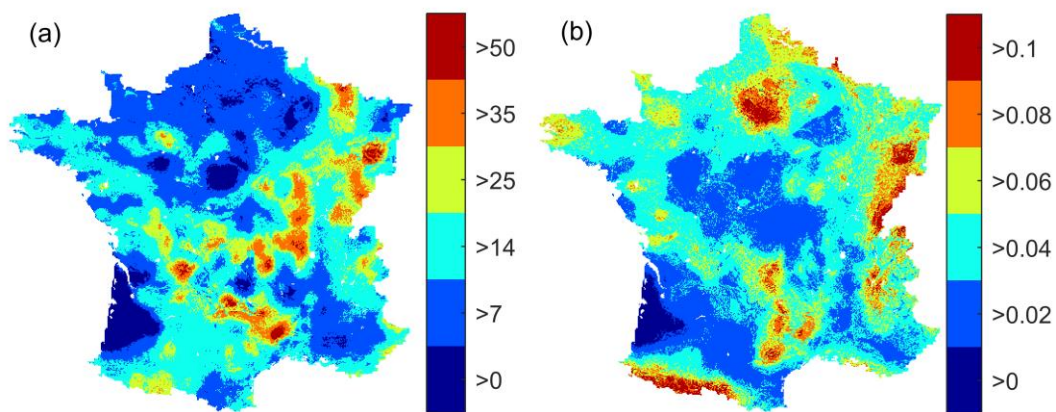
573



574

575 **Figure 5:** (a) predicted map of expected arsenic concentrations; (b) predicted map of expected
576 mercury concentrations.

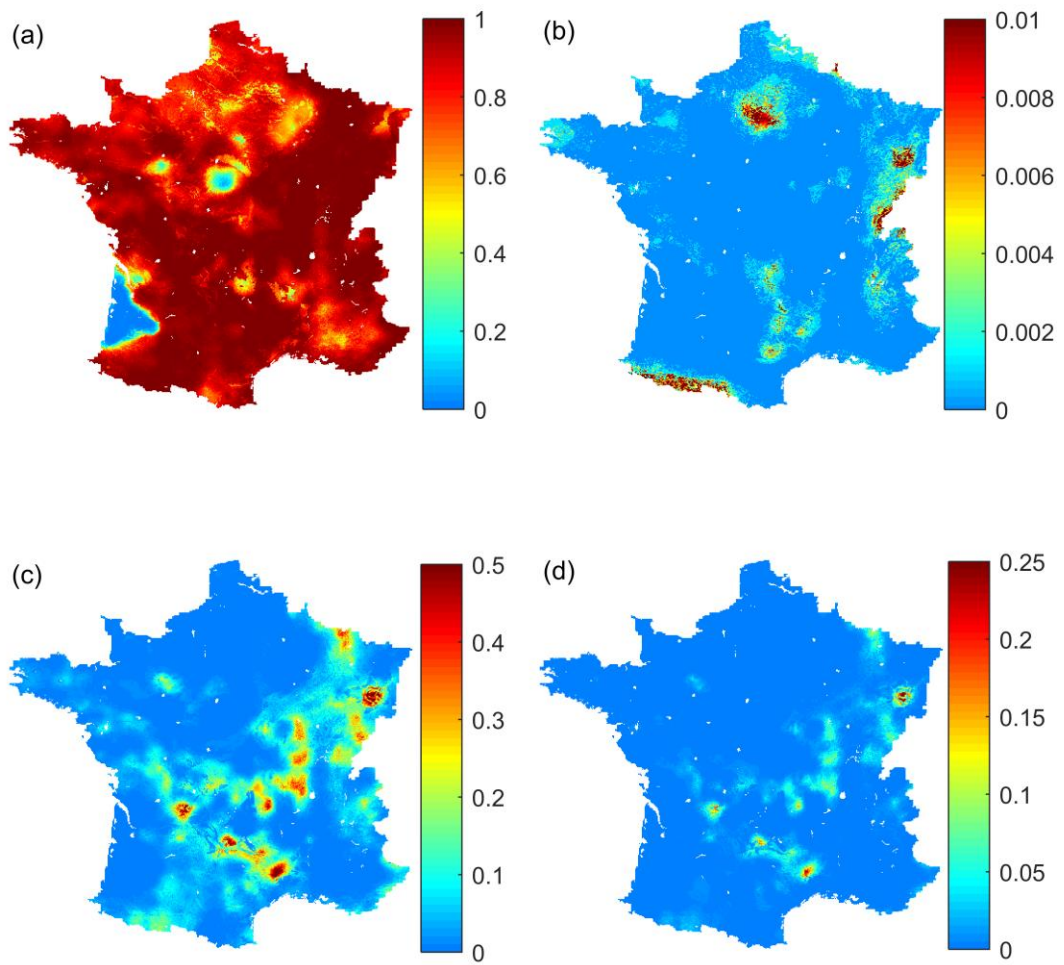
577



579

580 **Figure 6:** (a) categorical predicted map of expected arsenic concentrations (mg/kg); (b) categorical
581 predicted map of expected mercury concentrations (mg/kg).

582



584

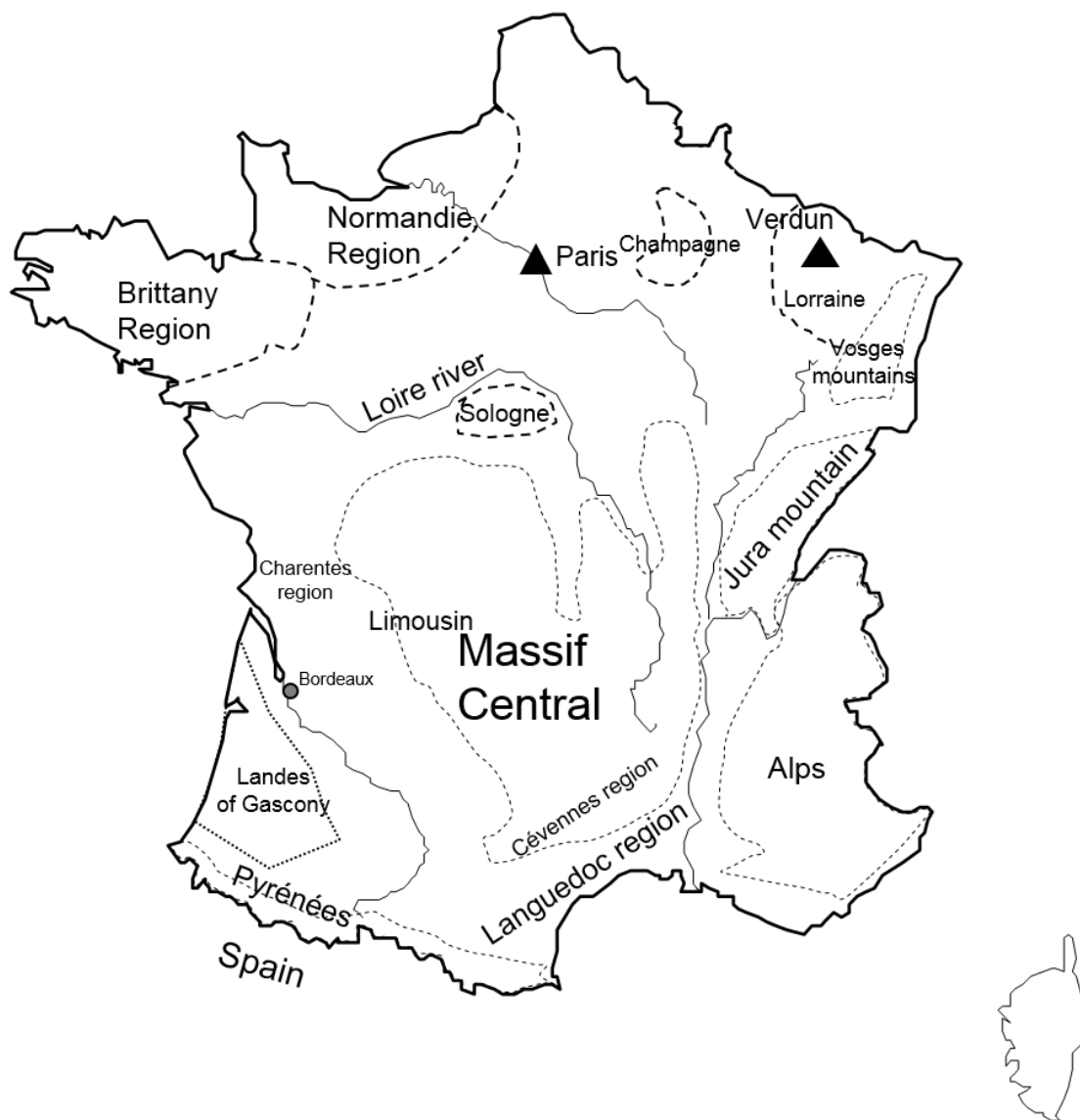
585

586 **Figure 7:** Predicted probabilities of exceedance of the Ministry of Environment of Finland (2007)
587 threshold and guidance values for metal/metalloids in soil. (a) arsenic concentration exceeding the
588 threshold value of 2 mg/kg; (b) mercury exceeding the threshold value of 0.5 mg/kg; (c) arsenic
589 exceeding the lower guideline value of 50 mg/kg; (d) arsenic exceeding the higher guideline value of
590 100 mg/kg.

591

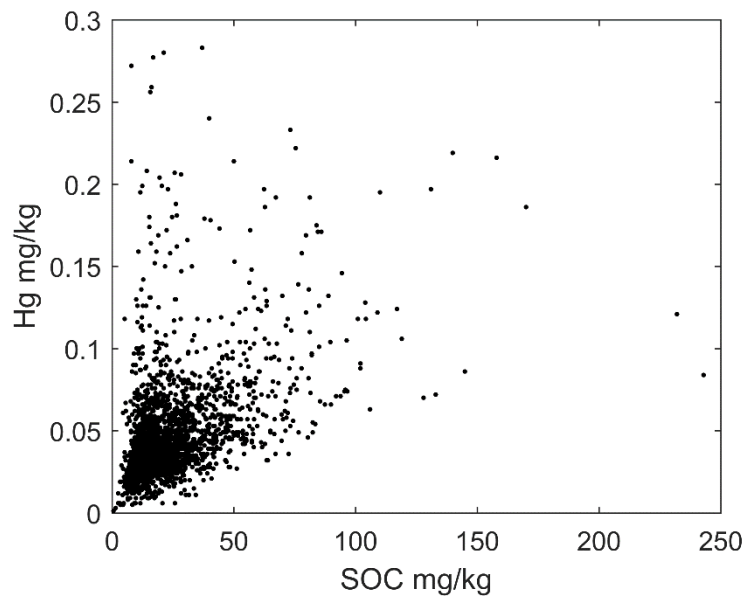
592

593



594

595 **Figure 8:** Relevant physical and geographical features in France.



596

597 **Figure 9:** Relationship between soil organic carbon and mercury concentrations (mg/kg) for RMQS
598 samples with mercury concentration less than 0.3 mg/kg.

599

600 **Tables**

601

Element	Threshold mg/kg	Lower guideline mg/kg	Higher guideline mg/kg
Arsenic	5	50	100
Mercury	0.5	2	5

602

603 **Table 1:** Ministry of Environment of Finland (2007) threshold and guideline concentrations for
604 arsenic and mercury in soils.

605

606

Element	<i>n</i>	Mean mg/kg	Median mg/kg	Min mg/kg	Max mg/kg	Skewness
Arsenic	2017	17.93	12.20	0.39	412.00	6.42
Mercury	2017	0.052	0.041	0.005	1.370	10.55

607

608 **Table 2:** Number of observations, *n*, and summary statistics for arsenic and mercury concentrations
609 in the RMQS survey.

610

611

Covariates	-L	No. of parameters	AIC	Mean (SSPE)	Median (SSPE)
c	0	6	12	1.00	0.32
c, pm	-29.9	14	-31.8	1.01	0.31
c, lu	-16.9	11	-11.7	1.00	0.30
c, pr	0.0	7	14.0	1.00	0.32
c, evt	-1.7	7	10.5	1.00	0.32
c, pm, lu	-44.1	19	-50.2	1.01	0.30
c, pm, pr	-30.0	15	-30.0	1.01	0.31
c, pm, evt	-31.1	15	-32.2	1.01	0.31
c, lu, pr	-17.6	12	-11.26	1.00	0.30
c, lu, evt	-17.6	12	-11.26	1.00	0.31
c, pr, evt	-1.9	8	12.2	1.00	0.32
c, pm, lu, pr	-45.3	20	-50.6	1.01	0.31
c, pm, lu, evt	-44.7	20	-49.3	1.01	0.30
c, pm, pr, evt	-31.6	16	-31.1	1.01	0.31
c, lu, pr, evt	-19.2	13	-12.4	1.00	0.30
c, pm, lu, pr, evt	-46.7	21	-51.3	1.01	0.31

612

613 **Table 3:** Statistics for estimated linear mixed models of arsenic. Covariates are constant (lu), parent
 614 material (pm), land use (lu), precipitation (pr), potential evapotranspiration (evt). Best fitting model
 615 is shown in bold. A constant has been added to the log-likelihood values such that the constant
 616 model has zero log-likelihood.

617

618

619

Covariates	-L	No. of parameters	AIC	Mean (SSPE)	Median (SSPE)
c	0	6	12.0	1.00	0.36
c, pm	-10.7	14	6.7	1.01	0.38
c, lu	-38.1	11	-54.1	1.00	0.36
c, pr	-11.6	7	-9.1	1.00	0.37
c, evt	-4.0	7	6.0	1.00	0.36
c, pm, lu	-50.4	19	-62.7	1.01	0.37
c, pm, pr	-20.9	15	-11.8	1.01	0.38
c, pm, evt	-13.6	15	2.8	1.01	0.38
c, lu, pr	-51.0	12	-78.0	1.01	0.36
c, lu, evt	-41.9	12	-59.7	1.01	0.36
c, pr, evt	-12.0	8	-8.1	1.00	0.37
c, pm, lu, pr	-62.1	20	-84.3	1.01	0.36
c, pm, lu, evt	-53.2	20	-66.5	1.01	0.36
c, pm, pr, evt	-21.3	16	-10.5	0.97	0.34
c, lu, pr, evt	-51.3	13	-76.6	1.01	0.35
c, pm, lu, pr, evt	-62.4	21	-82.8	1.01	0.36

620

621 **Table 4:** Statistics for estimated linear mixed models of mercury. Covariates are constant (c), parent
622 material (pm), land use (lu), precipitation (pr), potential evapotranspiration (evt). Best fitting model
623 is shown in bold. A constant has been added to the log-likelihood values such that the constant
624 model has zero log-likelihood.